Passive Optical Fast Frequency-Hop CDMA Communications System

Habib Fathallah, *Student Member, IEEE,* Leslie A. Rusch, *Member, IEEE, Member, OSA,*
and Sophie LaRochelle, *Member, OSA*

Abstract— This paper proposes an all-fiber fast optical frequency-hop code division multiple access (FFH-CDMA) for high-bandwidth communications. The system does not require an optical frequency synthesizer, allowing high communication bit rates. Encoding and decoding are passively achieved by strain-tunable fiber Bragg gratings. Multiple Bragg gratings replace a frequency synthesizer, achieving a hopping rate in tens of GHz. A main lobe sinc apodization can be used in writing the gratings to enhance the system capacity and the spectrum efficiency. All network users can use the same tunable encoder/decoder design. The simultaneous utilization of the time and frequency domains offers notable flexibility in code selection. Simulations show that the encoder efficiently performs the FFH spread spectrum signal generation and that the receiver easily extracts the desired signal from a received signal for several multiple access interference scenarios. We measure the system performance in terms of bit error rate, as well as auto-to cross-correlation contrast. A transmission rate of 500 Mb/s per user is supported in a system with up to 30 simultaneous users at 10^{-9} bit error rate. We compare FFH-CDMA to several direct sequence-CDMA systems in terms of bit error rate versus the number of simultaneous users. We show that an optical FFH-CDMA system requires new design criteria for code families, as optical device technology differs significantly from that of radio frequency communications.

Index Terms— Bragg grating, direct sequence code division multiple access (CDMA); frequency encoded CDMA, frequency hopping CDMA, optical multiple access protocols.

I. INTRODUCTION

CODE division multiple access (CDMA) is a highly flexible multiple access protocol with greatly varied applications, however, significant signal bandwidth expansion is required. Given the Terahertz pass band of optical fiber, the frequency spreading of the CDMA signal is no impediment, *provided it can be accomplished optically.* There are several methods that have been proposed to achieve passive optical CDMA. Chief among these is the use of optical delay lines and optical orthogonal codes for time domain coding of CDMA, and broadband sources or short pulses to accomplish frequency-encoded CDMA (FE-CDMA) [1]–[3]. We propose a new fast frequency hopped CDMA (FFH-CDMA) approach that has lower component cost, easier fabrication, and lower coupling losses. Applications include: local area networks, short-haul communications, smart photonic systems, switching, sensors multiplexing and on-board space and naval communications. The agility of modern radio transmitters to quickly change transmission frequencies for FFH-CDMA has no obvious corollary in optics. In [4] and [5], Kiasaleh proposed coherent slow frequency hopping (SFH, i.e., one frequency-hop per data bit) and very slow frequency hopping (one hop per packet of bits) for optical intersatellite communications. The bit rate was limited to a few tenths of Mb/s. In [6] and [7], we recently proposed a novel optical fast frequency-hop encoder/decoder employing a strain-tuned multiple fiber Bragg grating. Frequency hopping CDMA allows the simultaneous and efficient utilization of the time and frequency domains and does not require chip synchronization. The architecture of the encoder/decoder pair is an important feature of every CDMA system, the functionality of which should provide for an efficient encoding and correlation of the code sequences. We demonstrate via simulation that the proposed device can successfully perform the encoding/decoding operations, achieving low cross-correlation (or crosstalk) between different users' codes.

Fiber Bragg gratings are increasingly used to control and modify the amplitude and phase spectra of signals transmitted in lightwave systems [10]. Several applications have been demonstrated, including frequency control of semiconductor lasers, gain flattening of amplifiers, and add-drop filters. We propose a new application, using a series of Bragg gratings in a single fiber to generate CDMA hopping frequencies. Due to the linear "first in line, first reflected" nature of multiple Bragg gratings, the time frequency hopping pattern is determined by the order of the grating frequencies in the fiber. By use of piezo-electric devices, the order of the center frequencies of the Bragg gratings can be changed, effectively changing the hop pattern and therefore allowing for programmable codes.

In this paper, we analyze the achievable performance in terms of system capacity, and probability of error, auto-, and cross-correlation properties for various multiple access interference scenarios. The simultaneous utilization of the time and frequency domains in FFH-CDMA offers notable flexibility in the selection of codes, more easily satisfying the required quasiorthogonality (or transparency) between the

simultaneous users than previously proposed noncoherent direct sequence CDMA (DS-CDMA). It is important to note that code families previously developed for radio frequency (RF) communications are not directly applicable to an optical FFH-CDMA system. Our encoding device imposes special constraints on code design. We derive new design criteria unique to optical FFH-CDMA system. Some of these criteria are also useful for FE-CDMA schemes.

In [3], Ziemann and Iversen proposed acoustically tunable optical filters (ATOF) to implement FE-CDMA system. ATOF's can also be used for FFH-CDMA to improve performance over FE-CDMA. However, the ATOF, as well as other available spectral slicing integrated devices, suffer from insertion losses. In this regard, multiple fiber gratings appear to be a more promising implementation.

In Section II, we introduce the FFH-CDMA system model. We describe the proposed optical frequency hopping system in Section III and develop a suitable suboptimal family of codes adapted to this system. We also propose new code optimization and design criteria that better match the optical fiber medium. In Section IV, we analyze and numerically evaluate the performance of the proposed system in terms of probability of error. Simulations demonstrate the proposed encoding/decoding device successfully decodes the desired user's bits, and rejects the multiple access interference contribution. We also compare the performance of an FFH-CDMA system with some previously proposed noncoherent DS-CDMA systems.

II. FAST FREQUENCY-HOP CDMA SYSTEM

A. CDMA System Model

We consider a typical fiber optic CDMA communications network with transmitter and receiver pairs, i.e., K users share the same optical medium usually, but not exclusively, in a star architecture. Each information bit from user k is encoded onto a code sequence or "address"

$$c_k(t) = \sum_{j=1}^{N} d_{k,j} p_j(t - jT_c) \tag{1}$$

where N is the length of the code (or the number of chips per bit), $d_{k,j} \in \{0, 1\}$, for $1 \leq j \leq N$, is the jth chip value of the kth user's code and T_c is the chip duration. Let $\mathbf{c}_k = [d_{k,1}, d_{k,2}, \cdots, d_{k,N}]$ a vector representing the discrete form of the code. The chip signaling waveform $p_j(t)$, for $1 \leq j \leq N$, is usually assumed to be rectangular with unit energy. In our system $p(t)$ is the impulse response of a single grating. In our FFH system, the chip pulses are generated in different and disjoint frequency subbands (pulses with different colors). Each transmitter broadcasts its encoded signal to all the receivers in the network. The received signal is a sum of all the active users' transmitted signals

$$r(t) = \sum_{k=1}^{K} b_k c_k(t - \tau_k) \tag{2}$$

where $b_k \in \{0, 1\}$ and $0 \leq \tau_k \leq T_c$ for $k = 1, \cdots, K$, are the kth user's information bit and time delay, respectively.

The receiver applies a matched filter to the incoming signal to extract the desired user's bit stream. For notational simplicity, we assume that the desired user's signal is denoted by $k = 1$ and $\tau_1 = 0$. The matched filter output for bit duration T is thus

$$
\begin{aligned}
y &= \int_0^T c_1(t) r(t) \, dt \\
&= b_1 \int_0^T (c_1(t))^2 dt + \sum_{i=2}^{K} b_k \int_0^T c_1(t) c_k(t - \tau_k) \, dt \\
&= b_1 N + \mathrm{MAI}
\end{aligned}
\tag{3}
$$

where $T = NT_c$ is the duration of one data bit, and we have neglected the effects of quantum noise and thermal noise. The first term in (3) corresponds to the desired user; the second is multiple access interference (MAI). In most CDMA systems, the MAI is the most important noise source. For a large number of interfering users, the probability density function of the MAI is usually approximated to be Gaussian, appealing to central limit theorem arguments. To reduce the effect of the MAI, orthogonal (or nearly orthogonal) codes are required. For noncoherent DS-CDMA, different families of codes including so-called optical orthogonal codes (OOC's) have been developed with acceptable levels of crosstalk between users [13], [14].

B. FFH-CDMA System

In FFH-CDMA systems the available bandwidth is subdivided into a large number of contiguous frequency slots. The transmitted signal occupies one frequency slot in each chip signaling interval (T_c). A block diagram of the transmitter for a FFH spread spectrum system, as popularly implemented in radio frequency satellite communications, is shown in Fig. 1(a). The frequency synthesizer selects a frequency according to the output from the pseudo-random code generator. The synthesized frequency code is mixed with the data modulated carrier and transmitted over the channel. The modulation is typically either binary or M-ary FSK (frequency shift keying). In our system we use binary ASK (amplitude shift keying), as it is particularly suitable for optical communications. In the proposed FFH system, the modulator transmits power in the chip interval if the chip value is one; otherwise no power is transmitted. Similarly, Fig. 2(a) shows the block diagram of the receiver for a typical RF system. At the receiver, the pseudorandom frequency translation introduced at the transmitter is removed. A code generator, synchronized with the received signal, is used to control the frequency synthesizer; the resultant signal is then demodulated. A synchronization block is required in the receiver to acquire and maintain synchronism between the code generator and the desired received signal. The chip timing synchronization is extracted from the decoded, received signal. In Section III, we describe how our proposed optical-FFH system does not require a synchronization loop, notably simplifying the decoding operation. It should be noted that our encoding/decoding system is not suitable for slow frequency hopping (SFH) systems. In SFH, the frequencies must be tuned for every bit; thus the hopping rate would be limited
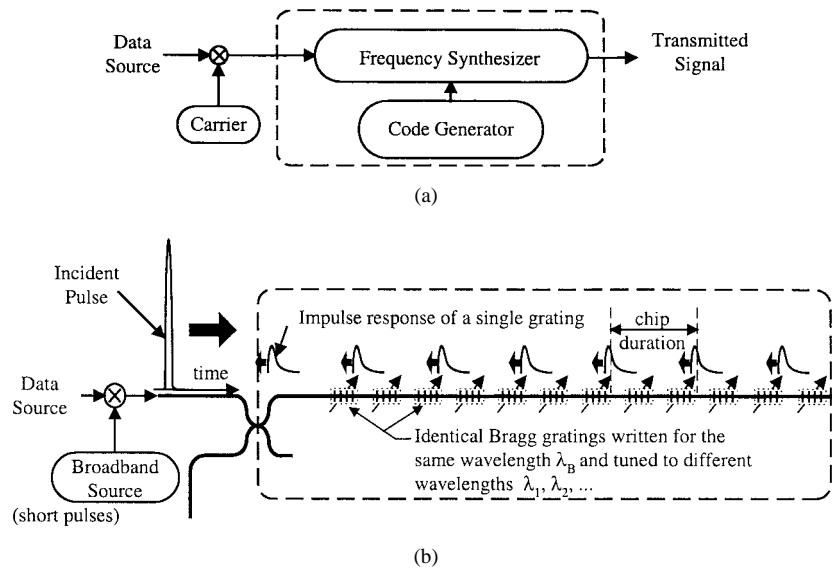
Fig. 1. (a) Block diagram of FFH-CDMA encoder and (b) proposed optical FFH-CDMA encoder.
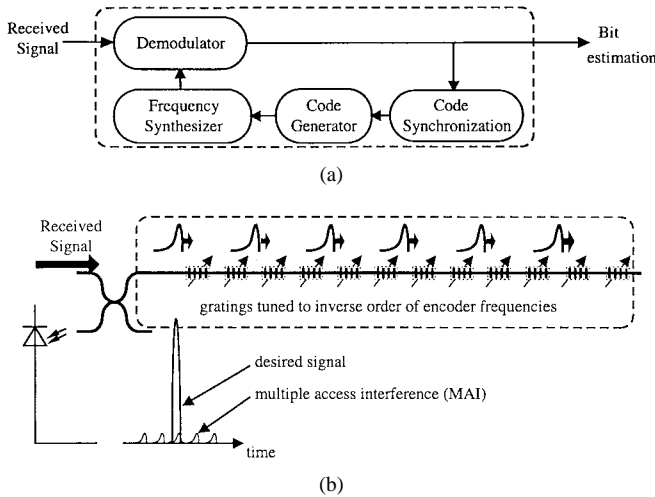

Fig. 2. (a) A block diagram of a the FFH-CDMA decoder and (b) proposed optical decoder.
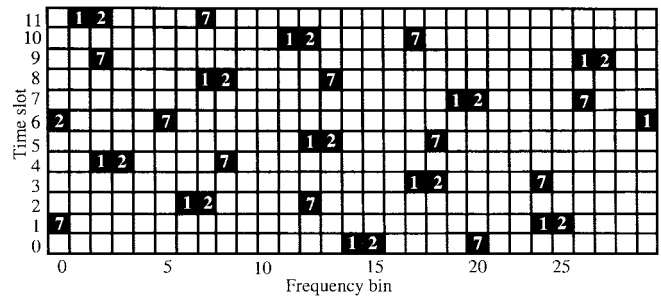

Fig. 3. Three hopping patterns in a system with 12 time slots and 29 hop frequencies; the black squares marked by 1, 2, and 7 represent the chip-pulses used by user number 1, 2, and 7, respectively.

by the tunability delay response of the gratings (in FFH the physical spacing between the gratings is the limiting factor as described in Section III-A). In the following section we address the coding issue, where we emphasize the particular code properties required by an optical FFH-CDMA system.

C. FFH-Coding

In FFH-CDMA, the lth chip pulse is modulated with frequency offset f_l about the carrier frequency f_c

$$f_t = \mathbf{h}(l)\frac{B}{q} \qquad l = 1, \cdots, N, \text{ and } 1 \le \mathbf{h}(l) \le q \quad (4)$$

where B is the available frequency bandwidth, $\mathbf{h}(l)$ is the placement operator (also called the frequency hop pattern), and q is the number of available frequencies. The placement operator is a sequence of N ordered integers determining the placement of frequencies in the N available time slots. Each user selects a set of N frequencies from a set of q

available frequencies $\mathbf{S} = \{f_1, f_2, \cdots, f_q\}$ where $N \le q$. A convenient way of representing a frequency hop pattern is through an $N \times q$ matrix representing the time and frequency plane (Fig. 3).

Most codes developed for radio frequency FFH-CDMA assume $N = q$. Only a few code families can be generalize to $N < q$; all are suboptimal. In our system the number N corresponds to the number of gratings written in the encoder. The number of available frequencies q is fixed by the tunability limit of the gratings (discussed further in Section III-D). In [15], Bin recently proposed a construction algorithm for a new family of codes with $q \ge N$. This family falls into the category of so-called one-coincidence sequences and is characterized by the following three properties: 1) all of the sequences are of the same length (here the length is equal to the number of gratings); 2) in each sequence, each frequency is used at most once; and 3) the maximum number of hits between any pair of sequences for any time shift equals one. For interested readers, we suggest a survey paper on one-coincidence sequences by Shaar *et al.* [16].

Let $\mathbf{c}_k(j)$ be the jth chip of code $\mathbf{c}_k$. As in any CDMA system, the users' codes are chosen to satisfy the following three fundamental conditions. First, the peak of the autocorrelation

function

$$R_m(s) = \sum_{i=0}^{N} c_m(i) c_m(i-s) \quad -N+1 \leq s \leq N-1 \quad (5)$$

should be maximized for each code; secondly the sidelobes of this function should be minimized and finally, the cross-correlation function

$$R_{m,p}(s) = \sum_{i=0}^{N} c_m(i) c_p(i-s) \quad -N+1 \leq s \leq N-1 \quad (6)$$

of each pair of sequences $\mathbf{c}_m$ and $\mathbf{c}_p$ should be minimized for all delays s. These conditions constrain the physical positioning of the gratings on the fiber as well as their bandwidth. The relative distances between the gratings must be chosen to satisfy a given level of auto- and cross-correlation between the codes. This distance in turn determines the achievable bit rate as discussed in Section III-A.

D. Signal-to-Interference Ratio and Probability of Error

Let $\overline{R}_{m,p}$ be the delay-averaged value of the cross-correlation between codes m and p. Then the variance of the cross-correlation between codes m and p is

$$\sigma_{m,p}^2 = \frac{1}{2N-1} \sum_{s=-N+1}^{N-1} \left(R_{m,p}(s) - \overline{R}_{m,p} \right)^2. \quad (7)$$

Since we do not know which codes will be active at any given time, we further average over all code pairs to arrive at $\sigma^2 = \overline{\sigma_{m,p}^2}$. With these definitions, the mean value of the MAI in (3) for K active users can be expressed as $\mu_{\mathrm{MAI}} = (K-1)\overline{R}_{m,p}$. Assuming the interfering users are statistically independent, the MAI has variance that can be approximated as [17]

$$\sigma_{\mathrm{MAI}}^2 = (K-1)\sigma^2. \quad (8)$$

The signal to interference can then be easily derived

$$\mathrm{SIR} = N^2 / (K-1)\sigma^2. \quad (9)$$

The output of the matched filter (3) is compared to the threshold $\eta = N/2 + \mu_{\mathrm{MAI}}$ to decide if a bit was transmitted. Using the Gaussian assumption for the MAI, and also assuming the system is MAI limited (i.e., neglecting other noise sources) the probability of error for equiprobable data is given by

$$\begin{aligned}
P_e &= \mathrm{Prob}(y \geq \eta | b_1 = 0) \cdot \mathrm{Prob}(b_1 = 0) \\
&\quad + \mathrm{Prob}(y \leq \eta | b_1 = 1) \cdot \mathrm{Prob}(b_1 = 1) \\
&= \tfrac{1}{2}\{\mathrm{Prob}(y \geq \eta | b_1 = 0) + \mathrm{Prob}(y \leq \eta | b_1 = 1)\} \\
&= Q\left(N \Big/ \sqrt{(K-1)\sigma^2} \right) = Q\left(\sqrt{\mathrm{SIR}} \right) \quad (10)
\end{aligned}$$

where

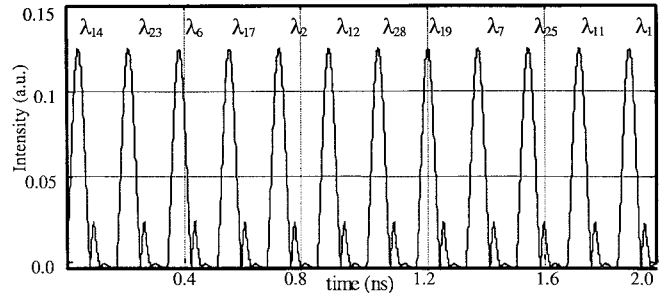$$Q(x) = \frac{1}{\sqrt{2\pi}} \int_x^{+\infty} e^{-u^2/2} \, du.$$

Fig. 4. Reflected series of pulses for placement operator [14 23 6 17 2 12 28 19 7 25 11 1]. These pulses correspond to the squares marked by 1 in Fig. 3, i.e., for user number 1. λ_{14} is the first wavelength transmitted and λ_{23} is the second, etc.

In this paper, we analyze only the performance degradation due to the presence of multiple access interference. The effects of quantum noise and thermal noise are neglected. The interferometric beat noise effect between frequency slices is not addressed here [8], [9]. In the theoretical calculation of the variance of the multiple access interference (7) and (8) we assumed chip synchronization, while for simulation we considered an asynchronous system. In a positive system the exact variance of MAI with arbitrary timing delays between users is less than its variance in a chip synchronous case. Salehi et al. [17] used this to demonstrate that synchronous DS-CDMA offers an upper bound on the exact probability of error

$$P_e(\text{exact}) \leq P_e \text{ (chip synchronous case)}. \quad (11)$$

This relationship holds for one-coincidence sequences, hence, is also true for the proposed optical FFH-system.

III. SYSTEM DESCRIPTION

A. The Encoding–Decoding Device

An optical FFH signal conforming exactly to the functional block diagram in Fig. 1(a), requires an optical frequency synthesizer with very precise frequencies and a high hopping rate. Practical frequency synthesizers however, have very limited frequency hopping rates. Even in radio frequency communications, the frequency synthesizer rate is the major limitation of system performance and directly affects the system cost. In our approach, we avoid all these requirements. As shown in Fig. 1(b), our encoding device consists of a series of Bragg gratings all written at the same wavelength λ_B [10] (also referred to as the Bragg frequency). Each grating can be tuned independently using piezoelectric devices to adjust the Bragg wavelength from λ_B to a given wavelength defined by the corresponding placement operator. One advantage of this approach is that only one phase mask is needed to write any encoder or decoder (reconfigurable codes). The tuning of each device will determine the code used. Note that the tuning time only affects link setup time and does not limit the bit rate.

The gratings will spectrally and temporally slice an incoming broadband pulse into several components as demonstrated by Chen et al. [12]. As illustrated in Fig. 4, each grating contributes a single reflected pulse. Pulses are equally spaced
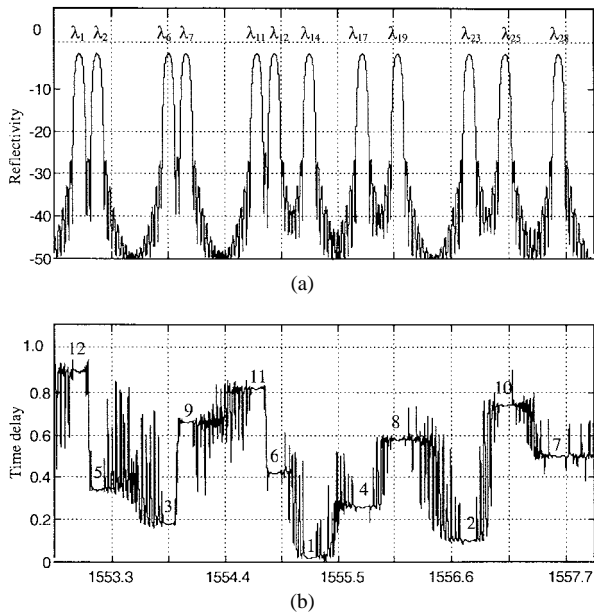
Fig. 5. (a) Reflected spectrum corresponding to the reflected series of pulses of Fig. 4 and (b) the group delay for each frequency bin. The marks 1–12 show the transmission order of the wavelengths, i.e., λ_1 is twelfth in the series, λ_2 is fifth, etc.

Fig. 6. Proposed FFH-CDMA encoder versus popular encoding devices: (a) DS-CDMA and (b) FE-CDMA.

at chip intervals T_c corresponding to the round-trip propagation time between two gratings, due to gratings being equally spaced. Fig. 4 corresponds to a particular user code with placement operator [14 23 6 17 2 12 28 19 7 29 11 1]. Fig. 5(a) depicts the transmitted spectral components corresponding to the same placement operator. Let L_c be the sum of one grating length and one spacing distance between adjacent grating pairs, c be the speed of light, n_{eff} be the average value of the effective refractive index; and n_g be the effective group index; then $T_c = 2n_gL_c/c$. The chip interval, the pulse duration, and the number of gratings will limit the data bit rate of the system, i.e., all reflections should exit the fiber before the next bit enters. Therefore, the total round trip time in a grating structure of N Bragg gratings is given by $2(N-1)L_cn_0/c$, effectively determining the bit duration T. The passage of the incident pulses through a grating of finite impulse response will necessarily lead to smearing of the pulse in time. Each grating bandwidth is constrained so that the time overlap of the reflected pulses does not degrade the cross-correlation function. The time delay between the frequency components of the simulated placement operator is presented in Fig. 5(b).

At the receiver, the pseudo-random frequency translation must be removed from the received signal as described in the block diagram [Fig. 2(a)]. In the decoder, the peak wavelengths are placed in reverse order of the peak wavelengths of the encoder to achieve the decoding function, i.e., matched filtering [Fig. 2(b)]. The proposed decoder removes the translation between the frequency components and realigns all chips into a single pulse. Note that the chip synchronization loop is avoided in this scheme.

B. Proposed FFH Encoder Versus DS and FE Encoders

Noncoherent direct sequence-CDMA is well studied in the literature [1]. An all optical implementation of this technique
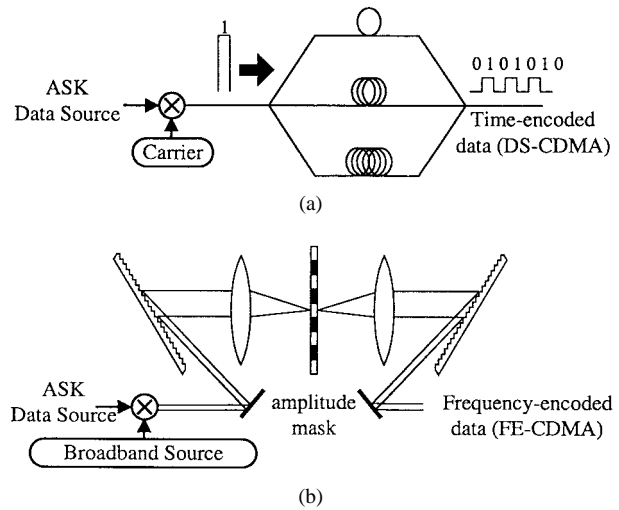
was based on a set of integrated delay lines as depicted in the Fig. 6(a). An incoming signal to this encoder is split into w independent paths. The number of paths, w, represents the weight of the code, i.e., the number of ones in a code. This technique led to the creation of optical orthogonal codes (OOC's) [13], [14].

Noncoherent frequency encoded-CDMA, originally proposed by Zaccarin and Kavehrad [2], is illustrated in Fig. 6(b). The diffraction grating achieves a spatial differentiation of the frequency spectrum into frequency bins. An amplitude mask is placed in the Fourier plane to imprint the code sequence onto the spatial frequency spectrum. The signal passes through the second diffraction grating to recombine the spectrum into a single signal, which is injected into the fiber for transmission.

Our proposed encoding device is a logical combination of these two encoders; the Bragg gratings achieve the frequency spectrum slicing and their positions in the fiber perform the same function as the delay lines of Fig. 6(a). The proposed communication system improves on previous systems by exploring the time-frequency diversity allowed by the encoding/decoding device. The high splitting loss inherent to the architecture of the DS-encoder is entirely avoided in the proposed FFH-encoder. The integrated FE-CDMA architecture can lead to notable insertion losses; our encoder does not suffer from this problem.

C. Apodization and Spectral Efficiency

In FFH-CDMA, the frequency components are assumed to have a rectangular shape. In our system, the gratings must be optimized to achieve near-rectangular spectrum slicing. This problem is known as bandpass (or bandstop filtering) in optical component design, e.g., as multiplexers–demultiplexers, WDM sources, etc. In our system, gratings with near-perfect rectangular band-pass filtering are required to achieve a high density of frequency bins in the available spectrum. The higher the number of available frequency bins, the higher the number of near-orthogonal codes (i.e., the larger the number of simultaneous users).
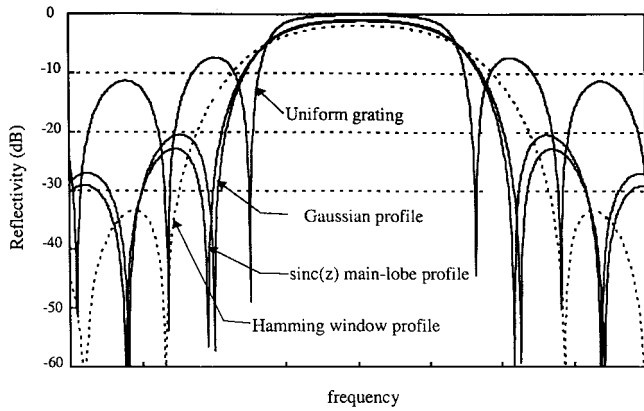
Fig. 7. Reflectivity of gratings for different apodization profiles.

Fiber Bragg gratings, usually produced by exposure of photosensitive fiber to ultraviolet light, have a refractive index that is spatially periodic along the fiber propagation axis. The Bragg grating operates as optical band-pass (or band stop filter). Only three parameters characterize the so-called uniform Bragg grating: the period Λ which determines the Bragg wavelength (the frequency of the peak grating reflectivity), the coupling coefficient κ_0 which reflects the strength of the grating (or the maximum reflectivity) and the grating length L which directly affects the reflection bandwidth as described in Section III-D.

Apodized Bragg gratings differ from the uniform grating in that their coupling coefficient varies along the propagation axis. The coupling coefficient as a function of position along the propagation axis, $\kappa_0(z)$, is called the apodization profile. Recently, Storoy *et al.* [11] demonstrated a very long grating with a sinc apodization with nearly ideal rectangular reflectivity. Recall that grating length and separation are limiting factors for the data bit rate. Near ideal rectangular reflectivity can be achieved only by using 1) a long grating with a sinc apodization including many side lobes, 2) the inverse Fourier transform of the raised cosine. We have examined several apodization profiles to achieve nearly disjoint and high-density frequency slices under the limited length constraint. Fig. 7 depicts the reflectivity of gratings with different apodization profiles: uniform, sinc_{ML} (sinc main lobe, i.e., sinc function with zero side lobes), Gaussian and Hamming window; all for 10 mm length and 220 m^{-1} coupling coefficient. In Appendix B, we report the mathematical definition of each function simulated. Among the four, the uniform grating has the narrowest main lobe (allowing for tighter frequency bins), but has the worst side lobes. The Hamming window has low side lobes, but an extremely wide main lobe. The Gaussian and sinc_{ML} profiles have similar main lobe widths, but the sinc_{ML} has lower side lobes, achieving -25 dB. We therefore opt for the sinc_{ML} apodization for our simulations. In Fig. 5(a), we depict the reflectivity of 12 gratings each with a sinc_{ML} apodization profile, i.e., one user code from Fig. 3. The central resonance wavelengths are selected allowing the first and second sidelobes of successive gratings to overlap, in order to increase bin density.

D. Tunability of Gratings

For uniform gratings of a given reflectivity, the reflection bandwidth is inversely proportional to the grating length. For example, the grating bandwidth between the two first zero crossings of the reflectivity spectrum is given by

$$\Delta\lambda_B = \frac{\lambda^2}{n_{\text{eff}}L}\sqrt{1 + (\kappa L/\pi)^2}$$

where κ is the coupling coefficient, L is the grating length, and λ is the peak wavelength. For a given fiber stretching ΔL, the shift in the peak Bragg wavelength $\Delta\lambda_s$ as a function of the applied strain is expressed by $\Delta\lambda_s = 0.8\lambda(\Delta L/L)$ [18]. Therefore the number of available frequency bins is related to the fiber stretching by

$$q = \frac{\Delta\lambda_s}{m\Delta\lambda_B} = \frac{0.8\Delta L n_{\text{eff}}}{m\lambda\sqrt{1 + (\kappa L/\pi)^2}}$$

where m is a coefficient that takes into account the excess bandwidth left on each side of the main reflection lobe. For typical values $\kappa L = 2$ (corresponding to 93% reflectivity) and $n_{\text{eff}} = 1.452$, the required stretching is $\Delta L \approx mq\lambda$. Tuning range will vary depending on the piezo-electric devices available for stretching; we consider a tuning range of $0 \leq \Delta L \leq 50$ μm which implies $0 \leq mq \leq 33$. For our calculations we selected parameters leading to a nominal data rate of 500 Mb/s, fixing the total round trip time in the grating structure to 2×10^{-9} s $= 2(N-1)L_c n_g/c$. Taking into account physical constraints in writing Bragg gratings (length L) and the spacing required between gratings to perform strain tunability, we selected $L = 10$ mm ($\kappa L = 2.2$) with 8 mm spacing as reasonable values. This leads to $N = 12$ for the number of gratings and a chip rate of $N \times 500$ Mb/s $= 6$ Gb/s. These numerical values correspond to the series of reflected pulses depicted in Fig. 4.

E. Code Design for Optical FFH-CDMA

Codes previously developed for frequency hopping in RF applications were mainly selected: 1) to reduce the Doppler effect; 2) to minimize the frequency synthesizer agility requirements; and 3) to reduce MAI in asynchronous systems. Also, most assumed that the number of available frequencies q is exactly equal to the number of chips (or hops) per bit N. For our proposal only criterion 3 applies and $N < q$. Furthermore, the maximum number of hops is determined by the maximum number of gratings N that can be written in a fixed fiber length dictated by 1) the required bit rate, 2) grating length, and 3) physical spacing required to allow tunability of gratings. The number of frequencies is dictated by the tunability limitation of the gratings. These points lead to new optimization criteria in optical frequency hopping code design.

Bin [15] recently proposed a novel FFH-code generation algorithm. These codes fall into the category of one-coincidence sequences introduced in Section II, and guarantee a minimum distance, d, between adjacent symbols (or pulses). For our system, this means that the reflected frequency bins from adjacent pairs of gratings, (leading to two reflected pulses adjacent in time), are separated by a specified minimum

number of bins. In our case, this reduces the effect of side lobes in the reflectivity of each grating. We describe the main steps of the algorithm in Appendix A. Using $q = 29$, and $N = 12$, we derive 29 one-coincidence sequences with $d = 8$, including $c_1 = [14\ 23\ 6\ 17\ 2\ 12\ 28\ 19\ 7\ 25\ 11\ 1]$ and $c_2 = [15\ 24\ 7\ 18\ 3\ 13\ 0\ 20\ 8\ 26\ 12\ 2]$. Fig. 3 illustrates the frequency-hop patterns of codes 1, 2, and 7. The example of reflectivity and delay time curves shown in Fig. 5 corresponds to the frequency-hop pattern of code 1.

F. New Codes Optimization Criteria

The proposed codes cannot be considered as optimal codes for fiber optic CDMA. Indeed, these codes were developed for mobile and satellite communications, and minimize cross-correlation in mobile radio communications due to the Doppler effect. In optical fiber communications the Doppler effect can be neglected, while dispersion must be accounted for. It has been recently demonstrated that Frequency-Encoding CDMA systems suffer from optical beat noise appearing between the frequency slices at the photodetector [8], [9], and our system may suffer similarly. The development of code families that are robust against fiber dispersion and beat noise and ignoring the Doppler effect is a relevant axis of research.

IV. PERFORMANCE ANALYSIS

A. Auto- and Cross-Correlation

To estimate the performance of the proposed FFH-CDMA encoder–decoder we calculate the auto- and cross-correlation functions for different numbers of simultaneous users. In Fig. 8(a), we present the auto and cross-correlation for a single interfering user (simulated with code 2 of Fig. 3). The autocorrelation has an easily identifiable peak compared to the cross-correlation function. Recall that the high autocorrelation peak is used by the receiver to position the time of the detection window for the desired signal. In the remaining time of the bit, i.e., outside the detection window, only the interference energy is present. This interference energy is useful for the receiver to dynamically estimate the number of active users, which in turn determines the detection threshold.[1]

In Fig. 8(b)–(d), higher numbers of interfering users (5, 10, and 15) are present, and the cross-correlation function presents higher peaks, but the autocorrelation peak remains easily distinguishable. The largest cross-correlation peak slightly exceeds half of the autocorrelation peak. This means that the maximum number of active users is roughly equal to half the code capacity. This is consistent with 16 simultaneous users (1 desired user +15 interferers) in a system with 29 unique codes available.

[1] In the code set used for this simulation, the different code pairs do not have the same number of shared frequencies; hence the interference energy is not proportional to the number of interferers. Optimized codes could minimize the variance of the number of coincidences between code pairs to improve threshold estimation. Similarly, in noncoherent DS-CDMA systems, preferred OOC families had code pairs with similar number of shared chips.
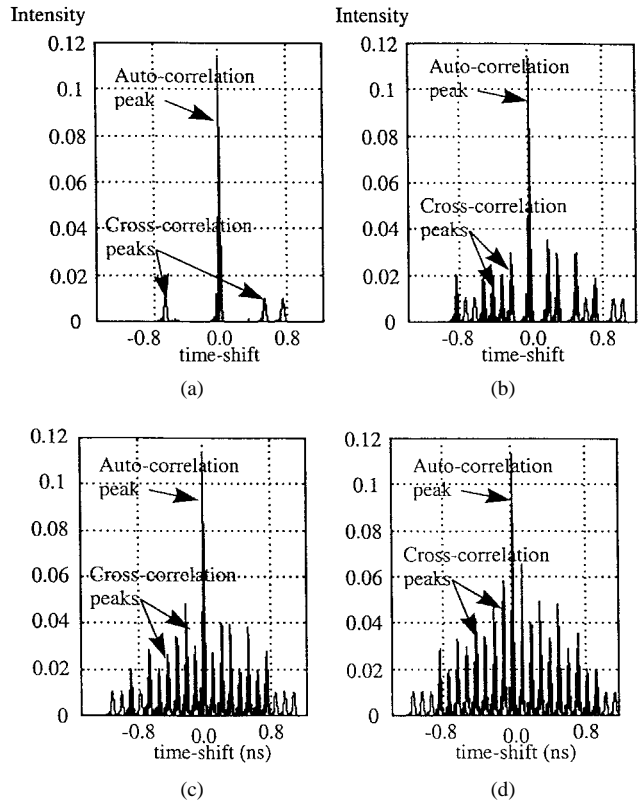

Fig. 8. Auto- versus cross-correlation functions for different numbers of simultaneous interferers: (a) only one interferer, (b) five simultaneous interferers, (c) ten interferers, and (d) 15 interferers.

B. Probability of Error

Simulations were run for Bragg gratings of length 10 mm, spacing of 8 mm and a main lobe sinc apodization. The average variance for codes implemented in the simulated gratings was calculated per (7). For $N = 12$, $q = 29$, Fig. 9 depicts the probability of error (10) versus the number of asynchronous simultaneous users; the interference contribution is assumed to have a Gaussian distribution. The upper bound (solid line) is derived assuming ideal reflectivity, and perfectly rectangular, disjoint, contiguous chip pulses. The simulated gratings (points) use nonideal reflectivity and noncontiguous chip pulses. As shown in Fig. 4, the chip pulse energy is not constant during the chip interval, but rather compressed in time, allowing for guard times between chip pulses. This arises from the physical spacing required between the gratings to allow tunability (see Section III-D). In systems applications where the encoding/decoding device is not required to be programmable, especially broadcast and sensors multiplexing applications, physical spacing between gratings can be reduced to enhance the system capacity and efficiency. Nonetheless, the spacing between chip pulses reduces the probability of coincidence between users in an asynchronous transmission system, and reduces the interference contribution and leads to better probability of error than a system with contiguous chip pulses. This phenomenon is illustrated in Fig. 9, where simulated gratings (points) with noncontiguous chip pulses have better performance than the ideal closely packed pulses (solid line). Thus, simulation results confirm good performance, even
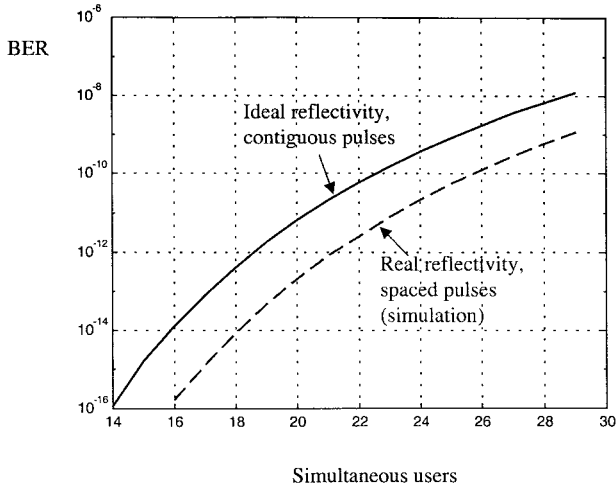
Fig. 9. Probability of error versus number of simultaneous users—true versus ideal reflectivity.
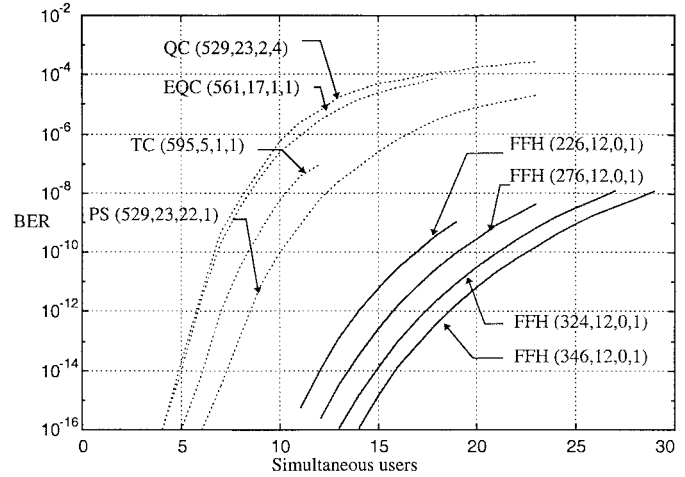

Fig. 10. Probability of error versus simultaneous number of users for FFH-CDMA (solid lines) and noncoherent DS-CDMA (dashed lines) with different families of codes PS, TC, QC, and EQC.

for nonideal reflectivity. Furthermore, selecting more suitable codes matching the new constraints of Section III-F can further reduce the probability of error.

C. Optical FFH-CDMA Versus Noncoherent DS-CDMA

In radio frequency systems, a FFH signal does not require the stringent synchronization inherent in DS spread spectrum signals. We compare the capacity of optical FFH-CDMA and noncoherent optical DS-CDMA in terms of simultaneous number of users, i.e., the number of codes with specified cross-correlation. Each family of optical orthogonal codes for DS-CDMA is usually characterized by the quadruple $(n, w, \lambda_a, \lambda_c)$ where n denotes the sequence length, w is the sequence weight, λ_a is the maximum of the autocorrelation sidelobes, and λ_c the maximum cross-correlation [13]. As FFH codes are two-dimensional the effective length of codes is $n = N \times q$, N being the number of gratings and q the number of available frequencies. In Fig. 10, we reproduce results from [14] which compare some DS-code families in terms of achievable probability of error as function of the simultaneous number of users and compare them with our suboptimal codes. FFH-codes for $N = 12$ and $q = 19, 23, 27$, and 29 corresponding respectively to quadruples $(12 \times 19 = 228, 12, 0, 1)$, $(12 \times 23 = 276, 12, 0, 1)$, $(12 \times 27 = 324, 12, 0, 1)$, $(12 \times 29 = 348, 12, 0, 1)$, clearly outperform DS-codes of even greater length, including prime sequences (PS), quadratic congruence codes (QC), extended quadratic congruence codes (EQC), and truncated Costas array codes (TC).

V. CONCLUSION

We propose and analyze a novel high bandwidth optical fast frequency-hop CDMA communication system. Encoding/decoding operations are performed passively, using an all-optical, all-fiber device. In a typical example of 500 Mb/s user data bit rate, a length 20 cm multiple Bragg gratings performs the function of a 6-GHz hopping-rate frequency synthesizer. Apodization of each grating is important to improve the reflectivity spectrum and hence enhance system capacity and

spectrum efficiency. Tunability using piezoelectric devices allows the programmability of the encoding/decoding device. We derived new code design criteria that better match requirements in optical fiber transmission medium. We proposed a suboptimal family of codes that guarantees a specific frequency separation between successive chip pulses, alleviating the effects of side lobes in the reflection spectrum. We addressed the receiver's ability to extract the desired signal for several interfering scenarios. Optical FFH-CDMA offers a large number of simultaneous users' codes with good transparency (low crosstalk) and, as demonstrated, optical FFH-CDMA easily outperforms noncoherent DS-CDMA for a given code length.

APPENDIX A

Let q be an odd integer, and define $N = 2k = q - 2d - 1$. Let $\mathbf{C} = (c_0, c_1, \cdots, c_{2k-1})$ be a permutation of $\mathbf{D} = (d+1, d+2, \cdots, q-d-1)$. Let $D_n(j) = \left(\sum_{i=n}^{(n+j-1) \bmod [2k]} c_i \right) \bmod [q]$, for $0 \leq n \leq 2k - 1$, and $2 \leq j \leq k$. We select $\mathbf{C}$ among the all the possible permutations of $\mathbf{D}$, which satisfies:

  1) $c_i + c_{i+k} = q$, and $0 \leq i \leq k - 1$
  2) For each j, $2 \leq j \leq k$, all the $D_i(j)$ are different for $0 \leq i \leq 2k - 1$.

If the vector $\mathbf{C}$ exists, it is called the generator sequence, and a set of q sequences are generated by $F_j = (D_0(1) + j, D_0(2) + j, D_0(31) + j, \cdots, D_0(2k) + j)$ where $0 \leq j \leq q - 1$, and "$+$" is modulo-q addition.

APPENDIX B

All apodization profiles are normalized to have the minimum equal to zero and the maximum equal to $\kappa_0 = 220$. We calculate the different profiles of Fig. 7 using

$$\kappa(z) = \kappa_0 \frac{g(z) - g_{\min}}{g_{\max} - g_{\min}}$$

where $g_{\max} = \max\{g(z)\}$ and $g_{\min} = \min\{g(z)\}$.

1) *For Gaussian Profile:* $g(z) = \exp[-G(z/L)^2]$, with $G = 1$.
2) *For Hamming Window:* $g(z) = [1 + H\cos(2\pi z/L)]/[1 + H]$, where $H = 0.55$. While not presented in Fig. 7, it was also considered.
3) *For* $\text{Tanh}(z)$ *Profile:* $g(z) = 1 + \tanh[\beta(1 - 2|2z/L|^\alpha)]$, with $\alpha = 3$ and $\beta = 4$.
4) *For Blackman Window Profile:* $g(z) = [1 + (1 + B)\cos(2\pi z/L) + B\cos(4\pi z/L)]/[2 + 2B]$, where $B = 0.18$.

ACKNOWLEDGMENT

REFERENCES

[1] J. Salehi, "Code division multiple-access techniques in optical fiber networks—Part 1: Fundamental principles," *IEEE Trans. Commun.,* vol. 37, pp. 824–833, Aug. 1989.

[2] D. Zaccarin and M. Kavehrad, "An optical CDMA system based on spectral encoding of LED," *IEEE Photon. Technol. Lett.,* vol. 4, pp. 479–482, Apr. 1993.

[3] O. Zeiman and K. Iversen, "On optical CDMA based on spectral slicing encoding with integrated optical devices," *SPIE Proc.,* vol. 2614, pp. 142–152, 1995.

[4] K. Kiasaleh, "Fiber optic frequency hopping multiple access communications system," *IEEE Photon. Technol. Lett.,* vol. 3, pp. 173–175, Feb. 1991.

[5] ——, "Performance of packet-switched fiber-optic frequency-hopping multiple-access networks," *IEEE Trans. Commun.,* vol. 43, pp. 2241–2253, July 1995.

[6] H. Fathallah, S. LaRochelle, and L. A. Rusch "Analysis of an optical frequency-hop encoder using strain-tuned Bragg gratings," in *Proc. OSA Topical Meeting on Bragg Gratings, Photosensitivity, and Poling in Glass Fibers and Waveguides: Applications and Fundamentals,* Oct. 1997, pp. 200–202.

[7] H. Fathallah, L. A Rusch, and S. LaRochelle "Optical frequency-hop multiple access communications system," in *Proc. 1998 IEEE Int Conf Commun.,* Atlanta, GA, June 1998, paper 36-2.

[8] E. D. J. Smith, P. T. Gough, and D. P. Taylor, "Noise limits of optical spectral-encoding CDMA systems," *Electron. Lett.,* vol. 31, no. 17, pp. 1469–1470, Aug. 17, 1995.

[9] E. D. J. Smith, R. J. Blaikie, and D. P. Taylor, "Performance enhancement of spectral-amplitude-coding optical CDMA using pulse-position modulation," *IEEE Trans. Commun.,* vol. 46, pp. 1176–1185, Sept. 1998.

[10] K. O. Hill and G. Meltz, "Fiber Bragg grating technology fundamentals and overview," *J. Lightwave Technol.,* vol. 15, pp. 1263–1276, Aug. 1997.

[11] H. Storoy, H. E. Engan, B. Sahgren, and R. Stubbe, "Position weighting of fiber Bragg gratings for bandpass filtering," *Opt. Lett.,* vol. 22, no. 11, June 1, 1997.

[12] L. Chen, S. Benjamin, P. Smith, and J. Sipe, "Ultrashort pulse reflection from fiber gratings: A numerical investigation," *J. Lightwave Technol.,* vol. 15, pp. 1503–1512, Aug. 1997.

[13] W. Chung, J. Salehi, and V. Wei, "Optical orthogonal codes: Design, analysis, and applications," *IEEE Trans. Inform. Theory,* vol. 35, no. 3, pp. 595–604, May 1989.

[14] V. Maric, M. D. Hahm, and E. L. Titlebaum, "Construction and performance analysis of a new family of optical orthogonal codes for CDMA fiber-optic networks," *IEEE Trans. Commun.,* vol. 43, pp. 485–489, Feb./Mar./Apr. 1995.

[15] L. Bin, "One-coincidence sequences with specified distance between adjacent symbols of frequency-hopping multiple access," *IEEE Trans. Commun.,* vol. 45, pp. 408–410, Apr. 1997.

[16] A. A. Shaar and P. Davies, "A survey of one coincidence sequences for frequency-hopped spread spectrum systems," *Inst. Elect. Eng. Proc.,* vol. 131, no. 7, pp. 719–724, Apr. 1984.

[17] J. Salehi and C. A. Brackett, "Code division multiple-access techniques in optical fiber networks—Part 2: Systems performance analysis," *IEEE Trans. Commun.,* vol. 37, pp. 834–842, Aug. 1989.

[18] M. Ibsen, B. J. Eggleton, M. Sceats, and F. Ouellette, "Broadly tunable DBR fiber laser using sampled fiber Bragg gratings," *Electron. Lett.,* vol. 31, no. 1, pp. 37–38, Jan. 1995.
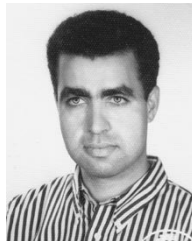
Habib Fathallah (S'96) was born in Ras Jebel, Tunisia, on March 14, 1969. He received the B.S.E.E and M.S.E.E degrees (with honors) from the National Engineering School of Tunis, 1994, a second M.S.E.E degree on CDMA wireless communications Université Laval, P.Q., Canada, in 1997. He is currently working towards the Ph.D. degree with the Centre dOptique Photonique et Laser (COPL) at Université Laval.

In his Ph.D. dissertation, he invented the all-optical/all-fiber FFH-CDMA system for LAN's, short-haul interconnects, fiber-to-the-home, and robust communications. His research interests include WDM fiber-optic communications, optical, and radio multiple- access techniques.

Leslie A. Rusch (S'91–M'94) was born in Chicago, IL. She received the B.S.E.E. degree with honors from the California Institute of Technology, Pasadena, in 1980, and the M.A. and Ph.D. degrees in electrical engineering from Princeton University, Princeton, NJ, in 1992 and 1994, respectively.

She is currently an Assistant Professor in the Department of Electrical and Computer Engineering at Université Laval, P.Q., Canada. She occupies a chair in optical communications jointly sponsored by the Natural Science and Engineering Research Council of Canada and QuébecTel. Her research interests include fiber optic communications, transient gain analysis of erbium-doped fiber amplifiers, wireless communications, spread spectrum communications, and code division multiple access for radio and optical frequencies.

Dr. Rusch is a member of the Optical Society of America (OSA).

Sophie LaRochelle received a Bachelor's degree in engineering physics from Université Laval, P.Q., Canada, in 1987 and the Ph.D. degree in optics from the University of Arizona, Tucson, in 1992.

From 1992 to 1996, she was a Research Scientist at the Defense Research Establishment Valcartier, where she worked on electrooptical systems. She is now an Assistant Professor in the Department of Electrical and Computer Engineering, Université Laval. Her current research activities are mostly focused on active and passive fiber optics components for optical communication systems including Bragg gratings, lasers, and amplifiers. She is also interested in nonlinear optics and tunable laser sources.

Dr. LaRochelle is a member of the Optical Society of America (OSA).